JACS
JOURNAL OF THE AMERICAN CHEMICAL SOCIETY
Article
pubs.acs.org/JACS

Evidence for Cardiolipin Binding Sites on the Membrane-Exposed Surface of the Cytochrome bc_1

Clement Arnarez,[†] Jean-Pierre Mazat,[‡] Juan Elezgaray,[§] Siewert-J Marrink,[†] and Xavier Periole*[,†]

[†]Groningen Biomolecular Sciences and Biotechnology Institute and Zernike Institute for Advanced Materials, University of Groningen, Nijenborgh 7, 9747 AG Groningen, The Netherlands

[‡]IBGC-CNRS UMR 5095 and Université Bordeaux Segalen, 1 rue Camille Saint-Saëns, 33077 Bordeaux, France

[§]Chimie et Biologie des Membranes et Nanoobjets, UMR 5248 - CNRS and Université Bordeaux 1, 2 rue Robert Escarpit, 33600 Pessac, France

Supporting Information

ABSTRACT: The respiratory chain is located in the inner membrane of mitochondria and produces the major part of the ATP used by a cell. Cardiolipin (CL), a double charged phospholipid composing ∼10−20% of the mitochondrial membrane, plays an important role in the function and supramolecular organization of the respiratory chain complexes. We present an extensive set of coarse-grain molecular dynamics (CGMD) simulations aiming at the determination of the preferential interfaces of CLs on the respiratory chain complex III (cytochrome bc_1, CIII). Six CL binding sites are identified, including the CL binding sites known from earlier structural studies and buried into protein cavities. The simulations revealed the importance of two subunits of CIII (G and K in bovine heart) for the structural integrity of these internal CL binding sites. In addition, new binding sites are found on the membrane-exposed protein surface. The reproducibility of these binding sites over two species (bovine heart and yeast mitochondria) points to an important role for the function of the respiratory chain. Interestingly the membrane-exposed CL binding sites are located on the matrix side of CIII in the inner membrane and thus may provide localized sources of proton ready for uptake by CIII. Furthermore, we found that CLs bound to those membrane-exposed sites bridge the proteins during their assembly into supercomplexes by sharing the binding sites.

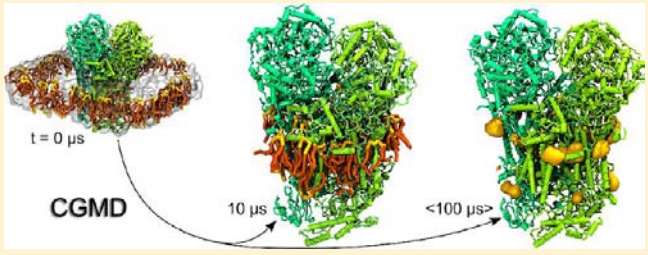

INTRODUCTION

Mitochondria are intracellular organelles, also referred to as the "power plants" of cells. They produce energy through the oxidative phosphorylation (OxPhos) system, which is embedded in their inner membrane. The OxPhos operates a series of electron transfers mainly carried out by three, large, membrane protein assemblies, the so-called "respiratory chain complexes" (complex I, CI, NADH quinone oxidoreductase; complex III, CIII, cytochrome bc_1; complex IV, CIV, cytochrome c oxidase) and by some small electron carriers (quinones and cytochrome c). The tortuous electron paths through the respiratory chain trigger the transport of protons from the inside (matrix) to the outside (intermembrane space, IMS) of the mitochondrial inner membrane, leading to an electrochemical gradient ultimately used by the complex V (ATP synthase) to synthesize ATP from ADP.

Cardiolipin (CL), the signature phospholipid of a mitochondrion, has broad and complex implications in the function of the OxPhos and other mitochondrial activities.[1,2] CLs are anionic phospholipids formed by two phosphatidyl groups bound by a glycerol. They compose 10−20% of the lipid of the mitochondrial inner membrane[3−7] but are also found in other parts of the mitochondria. CL deficiency is associated with numerous diseases[1,6,8] including the Barth syndrome[9] and heart failure.[10] Notably the formation, stability, and function of individual respiratory chain complexes[11,12] and of the supercomplexes they must form in order to function[13] strongly depend on the presence of CLs in the membrane environment.[12,14−19] Structural studies of complexes I,[20] III,[15] IV,[21] and V[22] from various organisms pointed to several CLs bound to the individual complexes, leading to the hypothesis about, for instance, their possible involvement in a proton uptake pathway in CIII[23] and in their assuring of the structural integrity of individual complexes.[22,23] CLs also associate with ADP/ATP protein carrier function.[24]

It is, however, unclear from the location of the CLs in the protein structures by which mechanism they might, for example, operate to "glue the respiratory chain together"[14,15] or make full use of their ability to trap protons.[25,26] Most cocrystallized CLs are indeed difficult to access from the bulk membrane as they are either deeply buried in cavities inside the protein or physically separated from the bulk by a specific subunit. It is likely that these CLs are tightly bound to the proteins and thus remain after protocols of protein purification, in which detergents are often used to wash away the lipid

Received: October 26, 2012
Published: January 30, 2013

   dx.doi.org/10.1021/ja310577u | J. Am. Chem. Soc. 2013, 135, 3112−3120

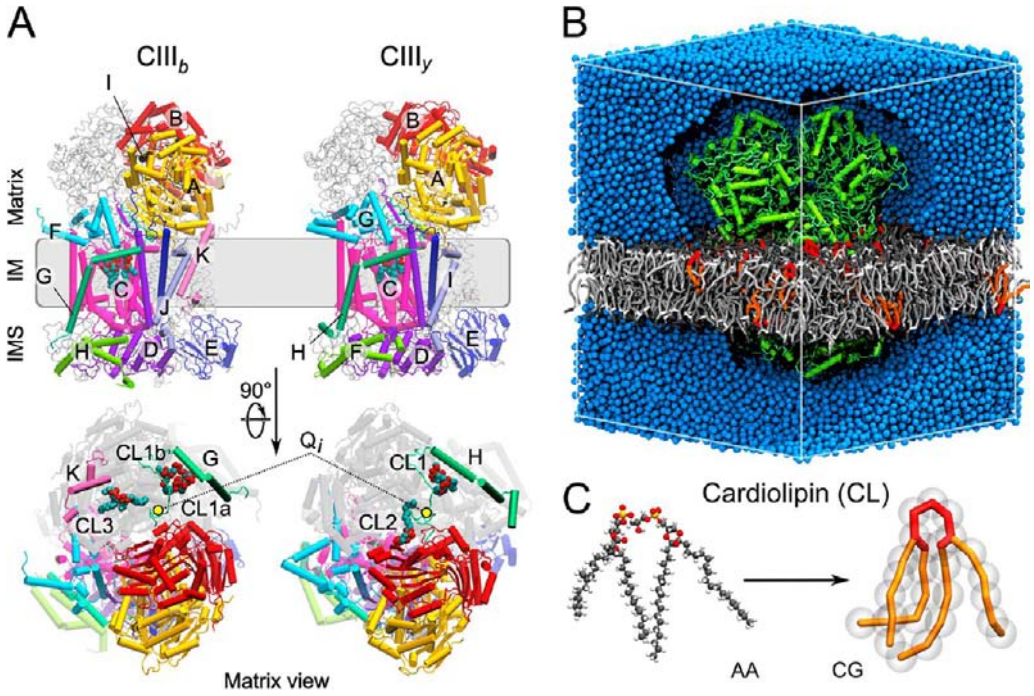

Figure 1. Structural characteristics of the wild-type cytochrome bc_1 (CIII) and of a cardiolipin (CL). (A) The 11 subunits (A–K) composing a bovine heart mitochondrial CIII$_b$ are shown in a cartoon representation. A chain-based color code is used on a monomer of both CIII$_b$ and the yeast CIII (CIII$_y$) such that equivalent subunits share the same color. The second monomer is shown in transparent gray. Subunits I and K of CIII$_b$ are missing in yeast. The inner membrane (IM) separating the matrix from the intermembrane space (IMS) is indicated in gray. In the matrix view (bottom row) the CLs known from structural studies (CL1–CL3) are depicted as balls and sticks in the transparent monomer together with some key subunits (G/H and K). The catalytic site Q_i (binding site of ubiquinol/ubiquinone on the matrix side) is indicated. (B) Simulation box for CIII$_b$-WT, with the protein shown in green, POPC molecules in gray/white, CLs in red/orange, and the aqueous phase in blue. Part of the aqueous phase is removed to ease the view of the system. The systems contains ~70000 CG beads. (C) Structure of a cardiolipin molecule in an all-atom (AA) and a coarse-grain (CG) representation.

membrane.[11] Here we explore the hypothesis according to which CLs present in the bulk membrane play an active role in the function of the respiratory chain in complement to the ones found within the protein structures.

To characterize the interaction between CLs found in the bulk membrane and CIII, we performed a series of coarse-grained molecular dynamics (CGMD) simulations of wild-type bovine and yeast CIII, as well as a couple of mutants, embedded in mixed palmitoyloleoyl-phosphatidylcholine (POPC)/CL membrane bilayers. MD simulations have been successfully used to explore the binding of lipids to a variety of membrane proteins.[27−34] Most of these studies rely on the CG MARTINI force field,[35,36] which we also used here. An overview of the current set of simulations is given in Table S1 (in Supporting Information [SI]), and the setup of the system is shown in Figure 1. The simulations reproduce the known CL binding sites and highlight key features of two subunits in controlling their stability and dynamics. In addition, the simulations reveal the existence of well-defined CL binding sites on the membrane-exposed protein surface of CIII. These new binding sites suggest possible involvement of CLs in the proton uptake by CIII. Moreover, supported by exploratory, simulations we discuss the mechanism by which these new CL binding sites might stabilize respiratory chain supercomplexes. The underlying principle of CL action should extend to other systems and might prove to be a generic mechanism by which lipids stabilize membrane protein complexes.

RESULTS

Identification of Six CL Binding Sites on Bovine Heart Cytochrome bc_1. The starting structure of our simulation consisted of the wild-type bovine CIII (CIII$_b$) dimer, including two of the cocrystallized CLs per monomer that are buried inside the protein (CL1a and CL1b, Figure 1A). On the basis of a 100 μs simulation (CIII$_b$-WT, Table S1 in SI) of this complex embedded in a POPC/CL membrane with a 17:1 molecular ratio (Figure 1B), we characterized the CL density around the protein. The average densities of CLs are shown in Figure 2A (see also video ja310577u_si_002.avi in SI) and demonstrate the existence of several preferential sites of interaction of CL with the protein. The densities were systematically reproducible in the various simulations performed (Table S1 in SI). We define CL binding sites as the locations with more than 5 times the bulk density, and symmetric densities must be observed on both monomers. Using this definition, six binding sites are found, and all are located on the matrix side of the protein although CLs are present in both layers of the membrane and uniformly visit both matrix and IMS sides of CIII. The sites are labeled I–VI as indicated in Figure 2A. The analysis of the sets of residues simultaneously in contact with a CL allowed the structural characterization of the binding sites shown in Figure 2B–F. Only sites I–IV are well-defined. Site V and VI are more dynamic, and a set of contacting residues could not be determined. Sites I and IV may be occupied by two CLs, and are therefore subdivided into Ia/Ib and IVa/IVb. Average occupation and CL residence time for each site are listed in Table 1. Details of the analysis methods are given in the SI.

dx.doi.org/10.1021/ja310577u | J. Am. Chem. Soc. 2013, 135, 3112−3120

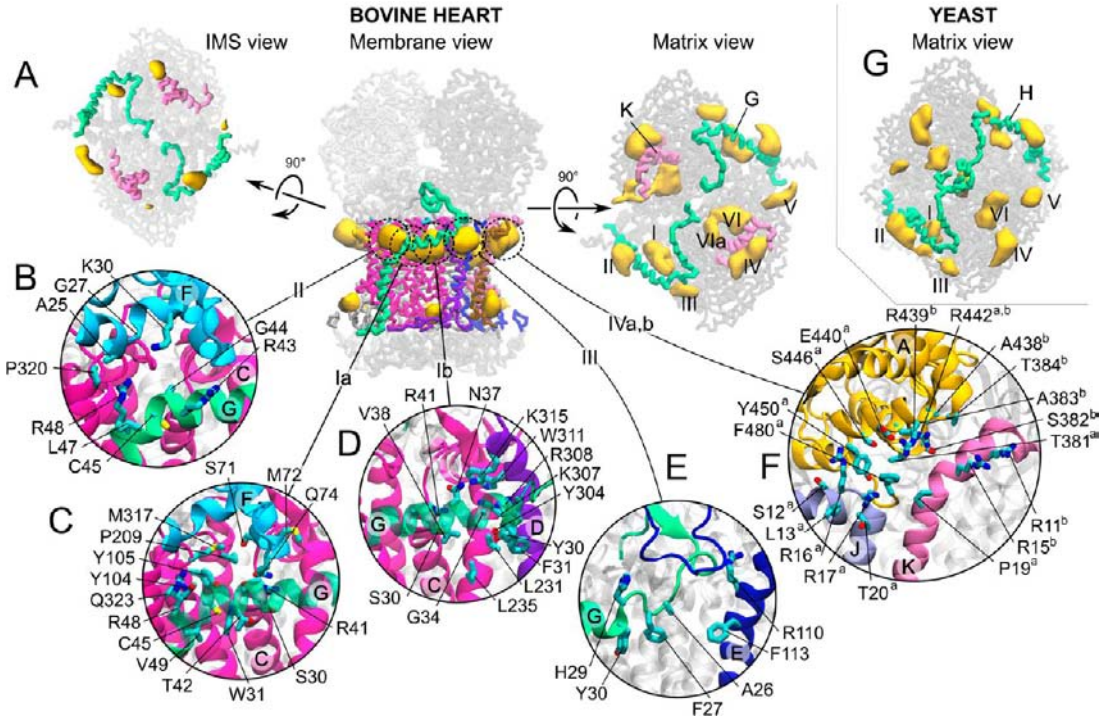

Figure 2. Cardiolipin (CL) binding sites of cytochrome bc_1 (CIII) extracted from a 100 μs CGMD simulation of the complex embedded in a CL/POPC membrane bilayer. (A) Intermembrane space (IMS), membrane side and matrix views of $CIII_b$ with the CL densities shown in yellow volume maps at an isovalue corresponding to at least 5 times the bulk density. The protein is shown in a shaded gray stick representation with the CL densities projected on top of them in the IMS and matrix views. In the membrane view the backbone of the transmembrane core of the protein is shown with the chain-based color code used in Figure 1. The subunits G and K are highlighted in the IMS and matrix views. (B–F) Detailed description of the CL binding sites I to VI, defined for $CIII_b$. The residues are numbered as follows: "residue^{subsite}". For each site, the subunits involved in the interactions with the CLs are depicted as colored cartoons, following the color code defined in Figure 1. The rest of the protein is shown in a transparent gray cartoon. (G) Matrix view of the CL densities extracted from a 20 μs CGMD simulation of yeast CIII embedded in a CL/POPC membrane bilayer.

Table 1. Occupation (Ξ) and Residence Time (θ, μs) of CL Binding Sites of the Wild-Type $CIII_b$, Averaged (aver) over 100 μs of CGMD Simulation ($CIII_b$-WT) for Both Monomers (mer 1/2)[a,b]

	site	Ia	Ib	II	III	IVa	IVb	V[c]	VIa[c]	VI[c]
Ξ	mer 1	0.99	1.01	0.91	0.69	0.63	0.73	0.3	<0.1	1.3
	mer 2	0.95	1.71[d]	0.96	0.66	0.91	0.71	<0.1	0.85	2.7
	aver	0.97	1.01	0.94	0.68	0.77	0.72	–	–	2.0
θ	mer 1	>100	>100	7.4	0.5	2.6	0.8	~1	<0.1	~20
	mer 2	3.4	1.0	3.5	2.3	1.4	0.9	<0.1	>100	>100
	aver	>100	>100	5.5	1.4	2.0	0.9	–	–	–

[a]The errors are ±0.02 and ±0.1 at most for the occupancies and residence times, respectively. [b]More details are given in Table S3 and in the SI. [c]The analysis is based on a qualitative definition of the sites in contrast to sites I–IV. [d]The motion of CLs in site Ib made the calculation inaccurate; it is not used in the average.

Site I corresponds to a site previously described in numerous crystal structures and associated with proton uptake[23] (site close to the catalytic center Q_i). It contains two CLs in bovine heart CIII and is located in an external protein cavity at the junction of the subunits C, D and F. Most contacts between the CLs and the protein are made with the core subunit C and subunits D and G (Figure 2A, C,D). The cavity is "closed" by the subunit G, which lays a helical segment on the membrane surface across the entire cavity. In the simulation the site is doubly occupied (Table 1) and the CLs, being present from the start, do not exchange with the bulk; their associated lifetimes are infinite on the time scale of our simulation. The structural integrity of this external cavity is further discussed below. Sites II and site III each contain a single CL and are located on the surface of the protein, surrounding site I (Figure 2A, B, E). They both strongly interact with the section of subunit G laying on the membrane surface (on the opposite side of site I): site II with its C-terminus and subunit F and site III with the N-terminus and subunit E. Site II is significantly more occupied (94%) than site III (68%). CLs are more strongly bound to site II than to site III, with a lifetime of 5.5 μs versus 1.4 μs (Table 1). Site IV binds two CLs and is located at the entrance of a large inner cavity in the core of the protein embedded in the membrane (Figure 2A). Sites IVa,b are connected and in both sites CLs interact strongly with the subunit A (Figure 2F). The rest of the CL contacts with the protein involve subunit J and K for site IVa and IVb, respectively. The two subsites have a similar occupancy (~70–80%) and exchange CLs on a time scale of 1–2 μs. Site V is located on the other side of the inner cavity entrance and although CL densities are observed at the

dx.doi.org/10.1021/ja310577u | J. Am. Chem. Soc. 2013, 135, 3112–3120

same location in most simulations of CIII they were slightly asymmetrical (Figure 2A) and the cluster analysis did not converge to a consistent set of residues. The dynamic behavior of subunit K (see below) may be hold responsible for this inconsistency. The occupancy level for site V is 30% and the binding time around 1 μs. Site VI corresponds to the inner cavity itself and contains up to three CLs. A first CL penetrates the inner cavity of one monomer quite early in the simulation and reaches the site VIa corresponding to the CL3 found in the crystal structure (PDB structure 1sqp;[37] see Figure 1A) after ~15 μs. This site stays occupied during the remainder of the simulation, giving rise to an occupancy of 85% (Table 1). Two additional CLs rapidly follow the first one in the cavity where they remain for the rest of the simulation. In the other monomer CLs also penetrate the cavity but are more dynamic and do exchange with the bulk CLs on a time scale ~15 μs (video ja310577u_si_003.avi and Figure S2 in SI). Averaged over both monomers, the occupancy level of the inner cavity is 2.0 CLs (Table 1). Additional description of the inner cavity is given below.

CL Binding Sites Are Conserved over Species. To probe the conservation of CLs binding sites on CIII over species we compare the binding sites found in bovine heart mitochondria to the ones found in yeast mitochondria. On the basis of the CL densities obtained from a 20 μs simulation performed on wild-type $CIII_y$ ($CIII_y$-WT, Table S1 in SI), we define six binding sites found on both monomers and labeled I_{CIIIy}–VI_{CIIIy} (Figure 2G and Figure S1 in SI). These CLs binding sites are virtually identical to the ones described above for bovine heart (Figure 2A, matrix view, vs Figure 2G). The regions of high CL density that relate to these six sites systematically show up at the same location of CIII in both species and involve analogous subunits. The similarities of the location of the sites found on membrane-exposed protein surfaces (sites II–V) in the two species is even more remarkable than for the ones buried in protein cavities (sites I and VI) and strongly suggest that these sites might have a function conserved across species.

It is important to make a few remarks. First, in yeast only one CL fills the site I in the crystal structures[38] and thus in the initial conformation of our simulation (CL1 in Figure 1A). On an extended 100 μs time scale an additional CL finds its way into the cavity of site I_{CIIIy} of one of the monomers after ~25 μs of simulation (video ja310577u_si_005.avi in SI). The penetration of the CL shows up as an additional density visible in Figure S1 in SI. In the other monomer the transmembrane section of the subunit G slightly collapses to occupy the extra space available, thus preventing the entry of an additional CL. Second, the CL density observed in the center of $CIII_y$ in between the two subunits, C, of the dimer corresponds to the position of a CL found in the crystal structure of the protein[38] (CL2 in Figure 1A). Third, the subunit homologous to bovine heart subunit K is missing in $CIII_y$. The lack of this subunit opens a wide access to the inner cavity of $CIII_y$ (Figure 1A). As a result, CLs penetrate the cavity and explore site VI much faster and diffuse more easily in the simulation of $CIII_y$ compared to that of $CIII_b$ (see videos ja310577u_si_003.avi and ja310577u_si_005.avi in SI).

Subunit G Important for the Structural Integrity of Catalytic Site I_{CIII}. The catalytic site I is buried in a cavity at the surface of CIII (Figure 2A, C, D, G). The experimental structures suggest that the subunits G in bovine heart and its homologous H in yeast physically separate the cavity from the bulk membrane. A helical segment of the subunit G (residues 30 to 46) in $CIII_b$ lays parallel to the membrane surface and interacts on one side with the CL head groups occupying the sites Ia,b and on the other side with the bulk lipids and CLs in sites II and III. Our simulations confirm this separation: lipids do not exchange between the site and the bulk membrane during the simulations. There is also no exchange in an additional simulation in which (two) POPC molecules replace the CLs within the site (simulations $CIII_{b/y}$-EmpCav, Table S1 in SI). Neither POPC molecules exchange with the bulk nor CLs enter the site to replace the POPC molecules.

To further investigate the possible protecting role of subunit G (H in yeast), simulations were performed with the transmembrane section of this subunit removed, leaving the site I accessible to the bulk ($CIII_b$-woG and $CIII_y$-woH, Table S1 in SI). Indeed, CLs spontaneously bind the site and dynamically exchange with the bulk in both bovine heart and yeast CIII simulations. On average about one CL binds to both bovine heart and yeast versions of CIII lacking the transmembrane segment of subunit G/H (Table S2 in SI). The penetration and stability of CLs in the site I_{CIIIy} is however sensitive to the presence of lysines in the binding site, as is evident from the simulation $CIII_y$-mut-woH (Table S1 in SI) of the triple mutant K288L/K289L/K296L of subunit D. In this case the CLs only marginally penetrate and bind to site I_{CIIIy} as shown by the almost null occupancy of the site (Table S2 in SI). This stabilization of the CL in site I_{CIIIy} by these three lysines was hypothesized earlier to rationalize the effects of this mutation on the structural and functional integrity on $CIII_y$ and its interactions with CIV.[17,23,39]

Subunit K Acts As a Gate for the Wide Inner Cavity of $CIII_b$. We have seen that lipid molecules (POPC and CL) penetrate the transmembrane inner cavity (site VI in Figure 2A) in both bovine heart and yeast CIII. We have also noted the increased dynamics by which CLs penetrate and explore the cavity in $CIII_y$ as compared to that in $CIII_b$, resulting from the absence of the subunit K in $CIII_y$. This difference suggests that the subunit K in $CIII_b$ restrains the dynamics of CLs within the transmembrane inner cavity and might thereby stabilize the binding of CLs. Here we describe an additional observation that further supports an important role of the subunit K in controlling CL entry into the inner cavity of $CIII_b$.

The subunit K is mobile and quite dynamic in the simulations (Figure 3A,B). The time course of a pair of distances between subunit K and the complex illustrates this behavior in the case of one monomer (Figure 3B and video ja310577u_si_003.avi in SI). The data shows that a quick "opening" of the cavity entrance allows for the subsequent penetration of three CLs into the inner cavity. Afterward the subunit K adopts a "closed" conformation similar to the one found in the crystal structure. At this point, the N-terminus of the subunit extends toward site V and completely obstructs the entrance of the cavity, thereby trapping the three CLs inside (Figure 3A,B). In the other monomer the subunit K also opens the access to the inner cavity, and CLs are able to go in. However, the cavity gets filled with three CLs only very late in the simulation and for a short time; closure of the gate is not observed (Figure S2 and video ja310577u_si_003.avi in SI). This behavior should not be confused with instability in the model but rather illustrates that the definition of force field (independent elastic networks for each subunit) gives enough flexibility to the model to allow reorientation of subunits (Figure 3A,B; Figure S2 and video ja310577u_si_003.avi in SI).

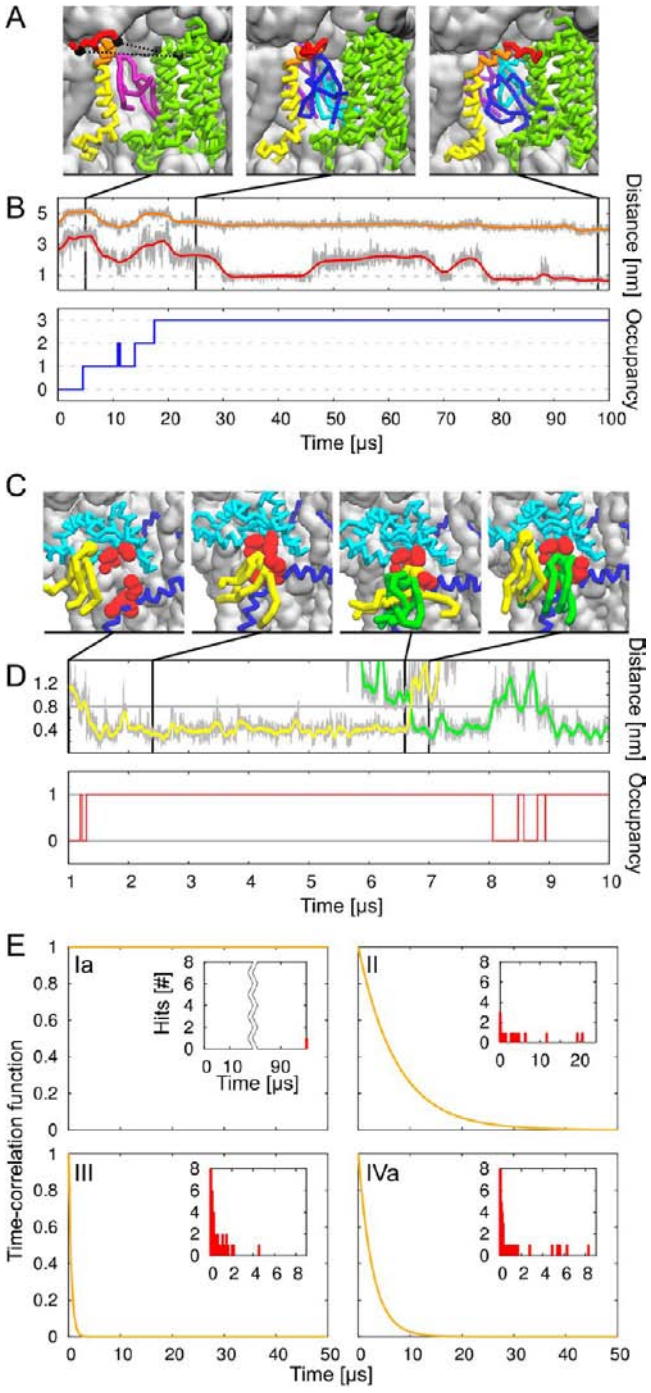

Figure 3. Dynamic features of CL binding to cytochrome bc_1 (CIII). (A, B) Opening and closing motion of subunit K at the entrance of the inner cavity, which is composed of subunit K (its N-terminus (red), a small helix segment lying on the membrane surface (orange) and the transmembrane section (yellow)), and the subunit C (light green). Panel A depicts (from left to right) three representative conformations of the subunit K and the CL content of the inner cavity extracted from the $CIII_b$-WT simulation: open with one CL, half open with three CLs, and closed with three CLs. CLs are shown in purple, blue, and cyan. The light-gray surface shows the rest of the protein. The distances between residue K:L2 and C:H309 (red), and K:R9 and C:F200 (orange) illustrate the motion of the subsections of subunit K (the color code follows that of the subsections); the occupancies of the inner cavity are shown in the top and bottom graphs of panel B. (C, D) Exchange of two CLs (yellow and green) in site II_{CIIIb} (red spheres) formed by subunits F (cyan) and G (blue). In panel C the exchange is depicted by four successive snapshots of the simulations $CIII_b$-WT. The panel D shows (top) the distance between the center of mass (COM) of the CLs headgroup and the COM of the site and (bottom) the occupation of site II_{CIIIb}. The colors in the distance plot correspond to the colors of the CL. (E) Time-correlation functions (orange curve) and distribution of residence times (red in the insets) for four sites of $CIII_b$. The time-correlation functions are used to extract the residence time of CL in the binding sites (Table 1) and are representative of the strength of CL binding.

DISCUSSION

Limitations of the Approach. In this work we used CGMD simulations to investigate the CL binding sites on the respiratory chain complex III, cytochrome bc_1. The ability of the approach to identify all the locations of the known CL binding sites (CL1−CL3 in Figure 1A) even when buried in cavities of the protein gives us confidence in its reliability. However, our simulations are still limited by the accessible simulation time of 100 μs. A hierarchy of binding times is observed, with many CL binding/unbinding events for some sites (e.g., more than 200 exchanges for site IVb) but only limited statistics for others (e.g., no unbinding events for site I). The time scale of different classes of CL exchange may be appreciated in Figure 3C−E. A complete overview of CL exchange events is given in the Table S3 in SI. We note that a qualitative level of convergence (i.e., densities shown in Figure 2) is reached after approximately 10 μs of simulation but a quantitative analysis of the lipid binding dynamics requires much longer time scales, especially pertaining to sites I and VI. Another important matter concerns the CG level of description, necessary to achieve the amount of sampling. To appreciate the importance of atomistic details for the description of CL binding sites, we performed a resolution transformation of the final configuration from our CG simulation $CIII_b$-WT to a full atomistic description. The 100 ns simulation following the transformation at the atomistic resolution confirmed the stability of all six CL binding sites of $CIII_b$. A structure file (PDB) of the system at the atomistic resolution is available upon request to the authors.

Validation of the binding strength of CLs, however, is not possible at the atomistic resolution level, and there is also no clear and precise experimental data that can be used to calibrate the interaction strength in our CG model. Especially the ability of the MARTINI force field to accurately represent salt-bridges could be questioned. In a recent study de Jong et al.[40] have probed amino-acid side-chain binding using the MARTINI force field and compared them to atomistic force fields. It was found that interaction strengths between charged residues (salt bridges) were well modeled by MARTINI in polar solvents typical of an aqueous environment or the interface between water and lipid head groups. In addition, in a similar study on CL binding to CIV,[41] we were also able to reproduce experimental binding sites of CL at the surface of the protein. Finally, in the recent work of Schmidt et al.,[42] the MARTINI force field predicted binding sites of PIP_2 lipids on a potassium channel, positions consistent with the current X-ray structures.

Biological Significance of Membrane-Exposed CL Binding Sites As Proton Carriers. A key result of our simulations is the prediction of several new CL binding sites on the membrane-exposed surface of CIII. We identified three main sites (II, III and IV in Figure 2) per monomer of CIII that are exposed to the bulk membrane and that were not known

dx.doi.org/10.1021/ja310577u | J. Am. Chem. Soc. 2013, 135, 3112−3120

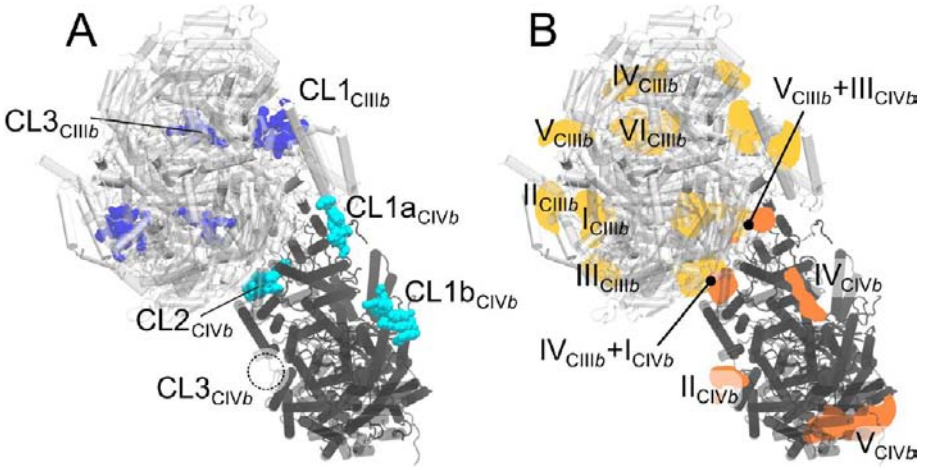

Figure 4. Matrix view of a III_2–IV supercomplex formed within a 5 μs self-assembly simulation of one CIII dimer (light gray) and two CIV (dark gray) of bovine heart mitochondria. (A) Experimental positions of CLs (dark blue for $CIII_b$, cyan for CIV_b).[37,63] The position of the $CL3_{CIVb}$ is as predicted by Sedlák et al.[64] (B) CL densities extracted from the simulations of isolated complexes ($CIII_b$-WT, Figure 2A and CIV_b-WT, Figure S4 in SI and reference 41) are shown in yellow and orange, respectively. The matrix (upper) parts of the complexes were made transparent to ease the visualization of the densities.

from the crystal structures. Another potentially relevant site (V in Figure 2) was observed but the mobility of subunit K prevented a precise definition. The use of protocols to purify proteins in which detergents often wash away lipids that are exposed to the bulk membrane can easily rationalize the absence of bound CLs in these additional sites in the crystal structures. Analysis of the distribution of residues in contact with the CLs show that, in general, the binding sites are enriched in positively charged residues; arginine notably, constituting around one-third of the sites (Figure S3 in SI). This behavior is consistent with the negative charge of cardiolipins. However, the salt bridges formed between CL and arginine in the membrane-exposed sites occur near the water/membrane interface and are presumably not strong enough to prevent their removal in the crystallization process.

The similarity of the main three membrane-exposed binding sites in bovine heart and yeast CIII is quite remarkable and suggests an important function. CLs have been associated with the proton transport activity of the respiratory chain complexes but the exact mechanism by which they operate is still unclear. They may be part of the proton uptake pathway[23] or supply the membrane water interface with a high proton buffering capacity[43] by using their ability to act as a proton trap.[25,26] In that context the CL binding sites, which are all found on the side of the proton uptake (matrix side of the protein), may well serve as proton sources. Previous simulations of CL binding to CIV indicate a similar potential role.[41] These protein bound CLs may define the precise location of proton uptake and subsequent delivery to the pumping process. The new membrane-exposed CL binding sites on CIII are likely to complement other binding sites described earlier. Notably sites II and III on the protein surface enclose site I that lies buried in the external cavity and which was associated with a proton uptake pathway.[23] The CLs identified in the inner cavity (site VI) may also have an active role in the proton uptake; site VIa was described earlier.[23,37,44] Further investigation is needed to define the exact role of these new CL binding sites in the proton uptake/release activity of CIII. We also note that one might expect an effect of CLs on the binding of the quinone molecules, whose binding sites are located in close vicinity of CL binding site I. Arias-Cartin et al.[45] have recently described a lack of binding of the quinones molecules in the absence of CLs in the membrane. The absence of CL was interpreted by a structural destabilization of a nearby heme center involved in quinone binding.

Biological Role of CLs in the Stabilization of Supercomplexes. Respiratory chain complexes self-organize into supramolecular structures called respiratory "supercomplexes" or "respirasomes".[13,46–48] Numerous experimental studies have shown the existence of supercomplexes consisting of CIII and CIV.[49] The formation and stability of these supercomplexes strongly depends on the presence of CLs in the membrane environment.[12,14–19] It is very tempting to speculate on the mechanism by which the membrane-exposed CL binding sites on CIII, revealed by the simulations, may relate to this stabilizing effect. The presence of CLs at specific locations of the protein surface might prevent the binding of potential partners at that same location ("protective mode") or the CL binding sites might define the actual location at which the proteins interact and CLs would be shared and glue the proteins together ("bridging mode"). To probe the mode of action CLs use to stabilize supercomplexes, we embedded a dimeric $CIII_b$ and two CIV_b with their first shell of bound lipids (POPCs and CLs) in a pre-equilibrated bilayer. A set of ten self-assembly simulations was run as explained in the SI Appendix. The data systematically show supercomplex formation with CLs at the interface between the complexes. A typical example of a CIII–CIV supercomplex is shown in Figure 4. The CLs binding sites are conserved on each of the complexes (the binding sites of CIV are given in Figure S4 in SI) and are shared in the supercomplex formed, suggesting that CLs operate according to a bridging mode. In the course of the formation of protein contacts the complexes first form an encounter complex in which CL binding sites are the main zones of contacts. Slow and small rearrangements of the relative orientation of the proteins follow this first encounter together with the release of the excess of CLs in the binding sites.

The relative orientation of the complexes in the supercomplexes formed in the simulations is in a few cases similar to the one derived from electron density maps obtained by cryo-electron microscopy (EM). The structure shown in Figure 4 is an example of a supercomplex with a similar orientation as the

dx.doi.org/10.1021/ja310577u | J. Am. Chem. Soc. 2013, 135, 3112–3120

most recent model proposed by Dudkina et al.[48] and Althoff et al.[50] An earlier model of heart bovine supercomplex proposed of Schäfer et al.[46] suggested a 180° rotation of the CIV relative to CIII but interacting on a similar face of CIII. None of the conformations obtained in the self-assembly simulation were comparable to this last model, nor to the model of the yeast supercomplex in which case the orientation of CIV is slightly different and interacts with another region of CIII.[49,51] The limited statistics of our self-assembly simulations restrict us to this very qualitative description, however.

The Role of Subunits in Protecting Catalytic CL Binding Sites. We find a pivotal role of the subunit G in $CIII_b$ (H in $CIII_y$) in protecting the catalytic CL binding site I. Our data show that, while this subunit is not necessary for CL binding to site I, it is of primary importance to preserve the structural integrity of the site. It prevents lipid (POPC and/or CL) from exchanging with the bulk membrane and stabilizes the two CLs bound. Interestingly, our data also point to the potential presence of two CLs in yeast CIII, although only a single CL is present in the crystal structures. A double occupancy of site I_{CIIIy} may be expected, considering that the space available in the cavity of bovine heart and yeast are similar (Figure S5 in SI). Site I of chicken CIII also contains two CLs.[52] Ongoing investigations will help resolve whether or not the site I contains two CLs in yeast.

We also find that, in yeast, D:K288, D:K289, and D:K296 are mandatory for the binding of CLs to site I_{CIIIy}. This result corroborates the earlier interpretation of the effect of these mutations on the catalytic activity of $CIII_y$,[23,39] namely the loss of activity being a consequence of the structural destabilization of the CLs bound to site I. One can easily extend the role of these lysines from the stabilization of the CLs bound to site I to the stabilization of subunit H (G in $CIII_b$) that strongly interacts with these CLs (Figure 2). A destabilization of the subunit H could explain the effect of these mutations on the stability of III–IV supercomplexes since subunit H has been suggested to be part of the interface.[15] In that context it is worth recalling the contribution of subunit H (G in $CIII_b$) to sites II and III, which might be involved in the interface between complexes.

The subunit K, present in $CIII_b$ and absent in $CIII_y$, is often missing in the crystal structures. Our simulations depict a very dynamic subunit K and suggest that in bovine heart it may act as a gate to the wide inner cavity (Figure 3A,B). In both $CIII_b$ and $CIII_y$ up to three CLs penetrate the inner cavity, but exchanges with the bulk are much more dynamic in $CIII_y$ than in $CIII_b$. In the case of $CIII_b$ the subunit K performs an opening/closing movement that controls the accessibility of the cavity (video ja310577u_si_003.avi in SI). Also notable is that, after a third CL has penetrated the cavity, the subunit physically closes the entrance of the cavity (Figure 3A,B). This event might be isolated and needs to be investigated in more detail. It is, however, quite possible that subunit K in $CIII_b$ has a similar CL-stabilizing role as we described for subunit G in $CIII_b$ (H in $CIII_y$) in relation to site I.

In summary, we have presented an extensive set of CGMD simulations that characterizes the preferential interfaces of CLs on the respiratory chain CIII of bovine heart and yeast mitochondria. We showed that CL binding sites in both buried protein cavities and membrane-exposed protein surfaces appear in a highly reproducible manner and are conserved over species. These binding sites open multiple new perspectives on the possible mechanism by which CLs might affect the catalytic activity of CIII but also of the respiratory chain in general. They notably suggest the existence of localized proton sources on the matrix side of the protein and anchors for the formation of supercomplexes. It will be interesting to study these hypotheses in the future both by computational and direct experimental methods.

METHODS

Protein Models. A model of cytochrome bc_1 (complex III, CIII) was built on the basis of the experimental structures from bovine heart mitochondria ($CIII_b$). We combined the *Protein Data Bank* (PDB) entries 1l0l,[53] 1sqb and 1sqq[37] and 2a06[54] to build a complete model. The CIII of yeast mitochondria ($CIII_y$) was taken from the PDB entry 3cx5[38] in which case the protein is fully resolved. CIII is functional in a dimer form and was thus simulated as such. In addition to the wild-type protein a couple of variants of the bovine and yeast CIII dimers were simulated (Table S1in SI). CLs consistently found inside protein cavities in the crystal structures (CL1a,b for $CIII_b$, and CL2 for $CIII_y$, see Figure 1A) were included in the simulations unless otherwise indicated. Cytochrome bc_1 contains three hemes and one iron–sulfur cluster per monomer. These molecules were not included in the simulations. The use of an elastic network (see below) in the CG model to control the protein fold compensates for their absence. More details about the models are given in the SI.

Mitochondrial Membrane. The mitochondrial membrane is a complex mixture of a large variety of lipid molecules. In our simulations, a mixture of POPC lipids and CLs models the mitochondrial membrane. The CL/POPC molecular ratio used in the simulations is between 1/17 and 1/19 (see Table S1 in SI). This CL content is in agreement with the composition reported for both bovine heart[4] and yeast mitochondria:[3] 20 and 16% of the total phospholipidic phosphorus, respectively. If we approximate the mitochondrial membrane to contain only PC lipids, this value would translate to a 1/16 CL/PC ratio.

System Setup. A list of the systems simulated is given in Table S1(in SI) together with some key characteristics. Each system was placed in a rectangular box containing a solvated and pre-equilibrated POPC/CL membrane patch. A typical system (e.g., $CIII_b$-WT, Figure 1B) contains the protein (4230 residues), a POPC bilayer (878 lipids) including 52 CLs and the aqueous phase (48,835 water beads—representing 195,340 real water molecules—and 118 sodium ions). For the supercomplex self-assembly simulations, we concatenated boxes containing the last conformation (100 μs, sites populated; see reference[41]) of each independent complex together. Random different initial velocities were taken for each simulation.

Force Field. The CG systems were described with the MARTINI CG force field for biomolecules (version 2.0),[35] its extension to proteins (version 2.1)[36] together with the ElNeDyn approach.[55] ElNeDyn maintains the secondary and tertiary structures of the subunits independently, so that domain motions (reorientation of subunits) are possible. Parameters for CLs were taken from the work of Dahlberg et al.[56] The MARTINI force field offers a near-atomic resolution in which small groups of atoms are represented by CG interaction sites. CGMD simulations based on this force field have been used in a number of large-scale studies probing lipid–protein interplay[30,32,57,58] and being able to identify specific lipid binding sites.[28] The CG system back-mapped to an atomistic resolution was described with the GROMOS 54a7 force field.[59]

Simulations Details. All simulations were performed using the GROMACS simulation package version 4.0.[60] The protein, membrane bilayer (POPC and CL), and aqueous phase (water and sodium ions) were weakly coupled[61] independently to an external temperature bath at 300 K. The pressure was weakly coupled[61] to an external bath at 1 bar using a semi-isotropic pressure scheme. The CG to atomistic resolution transformation followed the protocol described by Rzepiela et al.[62] Further details of the models, simulation protocols and limitations, as well as the methods used for analysis, are published as SI.

■ ASSOCIATED CONTENT

Supporting Information

Additional results, extended methods, additional tables and figures, additional references, and three videos. This material is available free of charge via the Internet at http://pubs.acs.org.

■ AUTHOR INFORMATION

Corresponding Author

x.periole@rug.nl

Notes

The authors declare no competing financial interest.

■ ACKNOWLEDGMENTS

X.P. thanks Thomas Haines, and X.P. and J.-P.M. thank Stéphane Ransac for insightful discussions. This work was supported by the CNRS (to J.-P.M., ANR-BBSRC 2207 BSYS 005 MitoScoP) and by The Netherlands Organisation for Scientific Research (NWO) (to X.P and S.J.M., ECHO.08.BM.041). We also acknowledge a DCCP Grant by The Netherlands National Computing Facilities Foundation (NCF).

■ REFERENCES

(1) Claypool, S. M.; Koehler, C. M. *Trends Biochem. Sci.* **2012**, *37*, 32−41.
(2) Osman, C.; Voelker, D. R.; Langer, T. *J. Cell Biol.* **2011**, *192*, 7−16.
(3) Jakovcic, S.; Getz, G. S.; Rabinowitz, M.; Jakob, H.; Swift, H. *J. Cell Biol.* **1971**, *48*, 490−502.
(4) Krebs, J. J.; Hauser, H.; Carafoli, E. *J. Biol. Chem.* **1979**, *254*, 5308−5316.
(5) Hoch, F. L. *Biochim. Biophys. Acta* **1992**, *1113*, 71−133.
(6) van Meer, G.; Voelker, D. R.; Feigenson, G. W. *Nat. Rev. Mol. Cell. Biol.* **2008**, *9*, 112−124.
(7) Daum, G. *Biochim. Biophys. Acta* **1985**, *822*, 1−42.
(8) Chicco, A. J.; Sparagna, G. C. *Am. J. Physiol. - Cell Physiol.* **2007**, *292*, 33−44.
(9) Schlame, M.; Ren, M. *FEBS Lett.* **2006**, *580*, 5450−5455.
(10) Saini-Chohan, H. K.; Holmes, M. G.; Chicco, A. J.; Taylor, W. A.; Moore, R. L.; McCune, S. A.; Hickson-Bick, D. L.; Hatch, G. M.; Sparagna, G. C. *J. Lipid. Res.* **2009**, *50*, 1600−1608.
(11) Qin, L.; Hiser, C.; Mulichak, A.; Garavito, R. M.; Ferguson-Miller, S. *Proc. Natl. Acad. Sci. U.S.A.* **2006**, *103*, 16117−16122.
(12) Claypool, S. M.; Oktay, Y.; Boontheung, P.; Loo, J. A.; Koehler, C. M. *J. Cell Biol.* **2008**, *182*, 937−950.
(13) Schägger, H.; Pfeiffer, K. *EMBO J.* **2000**, *19*, 1777−1783.
(14) Zhang, M.; Mileykovskaya, E.; Dowhan, W. *J. Biol. Chem.* **2002**, *277*, 43553−43556.
(15) Pfeiffer, K.; Gohil, V.; Stuart, R. A.; Hunte, C.; Brandt, U.; Greenberg, M. L.; Schägger, H. *J. Biol. Chem.* **2003**, *278*, 52873−52880.
(16) Gohil, V.; Hayes, P.; Matsuyama, S.; Schägger, H.; Schlame, M.; Greenberg, M. L. *J. Biol. Chem.* **2004**, *279*, 42612−42618.
(17) Zhang, M.; Mileykovskaya, E.; Dowhan, W. *J. Biol. Chem.* **2005**, *280*, 29403−29408.
(18) Claypool, S. M. *Biochim. Biophys. Acta* **2009**, *1788*, 2059−2068.
(19) Acehan, D.; Malhotra, A.; Xu, Y.; Ren, M.; Stokes, D. L.; Schlame, M. *Biophys. J.* **2011**, *100*, 2184−2192.
(20) Sharpley, M. S.; Shannon, R. J.; Draghi, F.; Hirst, J. *Biochemistry* **2006**, *45*, 241−248.
(21) Dale, M. P.; Robinson, N. C. *Biochemistry* **1988**, *27*, 8270−8275.
(22) Eble, K. S.; Coleman, W. B.; Hantgan, R. R.; Cunningham, C. C. *J. Biol. Chem.* **1990**, *265*, 19434−19440.
(23) Lange, C.; Nett, J. H.; Trumpower, B. L.; Hunte, C. *EMBO J.* **2001**, *20*, 6591−6600.
(24) Beyer, K.; Klingenberg, M. *Biochemistry* **1985**, *24*, 3821−3826.
(25) Kates, M.; Syz, J. Y.; Gosser, D.; Haines, T. H. *Lipids* **1993**, *28*, 877−882.
(26) Haines, T. H.; Dencher, N. A. *FEBS Lett.* **2002**, *528*, 35−39.
(27) Grossfield, A.; Feller, S. E.; Pitman, M. C. *Proc. Natl. Acad. Sci. U.S.A.* **2006**, *103*, 4888−4893.
(28) Stansfeld, P. J.; Hopkinson, R.; Ashcroft, F. M.; Sansom, M. S. P. *Biochemistry* **2009**, *48*, 10926−10933.
(29) Aponte-Santamaria, C.; Briones, R.; Schenk, A. D.; Walz, T.; de Groot, B. L. *Proc. Natl. Acad. Sci. U.S.A.* **2012**, *109*, 9887−9892.
(30) Schäfer, L. V.; de Jong, D. H.; Holt, A.; Rzepiela, A. J.; de Vries, A. H.; Poolman, B.; Killian, J. A.; Marrink, S. J. *Proc. Natl. Acad. Sci. U.S.A.* **2011**, *108*, 1343−1348.
(31) Domański, J.; Marrink, S. J.; Schäfer, L. V. *Biochim. Biophys. Acta, Biomembr.* **2012**, *1818*, 984−994.
(32) Periole, X.; Huber, T.; Marrink, S. J.; Sakmar, T. P. *J. Am. Chem. Soc.* **2007**, *129*, 10126−10132.
(33) Koivuniemi, A.; Vuorela, T.; Kovanen, P. T.; Vattulainen, I.; Hyvönen, M. T. *PLOS Comput. Biol.* **2012**, *8*, e1002299.
(34) Sengupta, D.; Chattopadhyay, A. *J. Phys. Chem. B* **2012**, *116*, 12991−12996.
(35) Marrink, S. J.; Risselada, H. J.; Yefimov, S.; Tieleman, D. P.; de Vries, A. H. *J. Phys. Chem. B* **2007**, *111*, 7812−7824.
(36) Monticelli, L.; Kandasamy, S. K.; Periole, X.; Larson, R. G.; Tieleman, D. P.; Marrink, S. J. *J. Chem. Theory Comput.* **2008**, *4*, 819−834.
(37) Esser, L.; Quinn, B.; Li, Y.-F.; Zhang, M.; Elberry, M.; Yu, L.; Yu, C.-A.; Xia, D. *J. Mol. Biol.* **2004**, *341*, 281−302.
(38) Solmaz, S. R. N.; Hunte, C. *J. Biol. Chem.* **2008**, *283*, 17542−17549.
(39) Wenz, T.; Hielscher, R.; Hellwig, P.; Schägger, H.; Richers, S.; Hunte, C. *Biochim. Biophys. Acta* **2009**, *1787*, 609−616.
(40) de Jong, D. H.; Periole, X.; Marrink, S. J. *J. Chem. Theory Comput.* **2012**, *8*, 1003−1014.
(41) Arnarez, C.; Marrink, S. J.; Periole, X. *Sci. Rep.* **2013**, DOI: 10.1038/srep01263.
(42) Schmidt, M. R.; Stansfeld, P. J.; Tucker, S. J.; Sansom, M. S. P. *Biochemistry* **2013**, *52*, 279−281.
(43) Haines, T. H. *Proc. Natl. Acad. Sci. U.S.A.* **1983**, *80*, 160−164.
(44) Palsdottir, H.; Hunte, C. *Biochim. Biophys. Acta* **2004**, *1666*, 2−18.
(45) Arias-Cartin, R.; Grimaldi, S.; Pommier, J.; Lanciano, P.; Schaefer, C.; Arnoux, P.; Giordano, G.; Guigliarelli, B.; Magalon, A. *Proc. Natl. Acad. Sci. U.S.A.* **2011**, *108*, 7781−7786.
(46) Schäfer, E.; Dencher, N. A.; Vonck, J.; Parcej, D. N. *Biochemistry* **2007**, *46*, 12579−12585.
(47) Bultema, J. B.; Braun, H. P.; Boekema, E. J.; Kouřil, R. *Biochim. Biophys. Acta, Bioenerg.* **2009**, *1787*, 60−67.
(48) Dudkina, N. V.; Eubel, H.; Keegstra, W.; Boekema, E. J.; Braun, H. P. *Proc. Natl. Acad. Sci. U.S.A.* **2005**, *102*, 3225−3229.
(49) Heinemeyer, J.; Braun, H. P.; Boekema, E. J.; Kouřil, R. *J. Biol. Chem.* **2007**, *282*, 12240−12248.
(50) Althoff, T.; Mills, D. J.; Popot, J.-L.; Kühlbrandt, W. *EMBO J.* **2011**, *30*, 4652−4664.
(51) Mileykovskaya, E.; Penczek, P. A.; Fang, J.; Mallampalli, V. K. P. S.; Sparagna, G. C.; Dowhan, W. *J. Biol. Chem.* **2012**, *287*, 23095−23103.
(52) Zhang, Z.; Huang, L.-S.; Shulmeister, V. M.; Chi, Y. I.; Kim, K. K.; Hung, L. W.; Crofts, A. R.; Berry, E. A.; Kim, S. H. *Nature* **1998**, *392*, 677−684.
(53) Gao, X.; Wen, X.; Yu, C.-A.; Esser, L.; Tsao, S.; Quinn, B.; Zhang, L.; Yu, L.; Xia, D. *Biochemistry* **2002**, *41*, 11692−11702.
(54) Huang, L.-S.; Cobessi, D.; Tung, E. Y.; Berry, E. A. *J. Mol. Biol.* **2005**, *351*, 573−597.
(55) Periole, X.; Cavalli, M.; Marrink, S. J.; Ceruso, M. A. *J. Chem. Theory Comput.* **2009**, *5*, 2531−2543.
(56) Dahlberg, M. *J. Phys. Chem. B* **2007**, *111*, 7194−7200.
(57) van den Bogaart, G.; Meyenberg, K.; Risselada, H. J.; Amin, H.; Willig, K. I.; Hubrich, B. E.; Dier, M.; Hell, S. W.; Grubmüller, H.; Diederichsen, U.; Jahn, R. *Nature* **2011**, *479*, 552−555.

(58) Periole, X.; Knepp, A. M.; Sakmar, T. P.; Marrink, S. J.; Huber, T. *J. Am. Chem. Soc.* **2012**, *134*, 10959−10965.
(59) Schmid, N.; Eichenberger, A. P.; Choutko, A.; Riniker, S.; Winger, M.; Mark, A. E.; van Gunsteren, W. F. *Eur. Biophys. J.* **2011**, *40*, 843−856.
(60) Hess, B.; Kutzner, C.; van der Spoel, D.; Lindahl, E. *J. Chem. Theory Comput.* **2008**, *4*, 435−447.
(61) Berendsen, H. J. C.; Postma, J. P. M.; van Gunsteren, W. F.; DiNola, A.; Haak, J. R. *J. Chem. Phys.* **1984**, *81*, 3684−3690.
(62) Rzepiela, A. J.; Schäfer, L. V.; Goga, N.; Risselada, H. J.; de Vries, A. H.; Marrink, S. J. *J. Comput. Chem.* **2010**, *31*, 1333−1343.
(63) Shinzawa-Itoh, K.; Aoyama, H.; Muramoto, K.; Terada, H.; Kurauchi, T.; Tadehara, Y.; Yamasaki, A.; Sugimura, T.; Kurono, S.; Tsujimoto, K.; Mizushima, T.; Yamashita, E.; Tsukihara, T.; Yoshikawa, S. *EMBO J.* **2007**, *26*, 1713−1725.
(64) Sedlák, E.; Robinson, N. C. *Biochemistry* **1999**, *38*, 14966−14972.